FEBS Letters 579 (2005) 6010–6016 FEBS 30020

Structural and morphological characterization of hemozoin produced by *Schistosoma mansoni* and *Rhodnius prolixus*

Marcus F. Oliveira[a,*,1], Stefan W. Kycia[b,1], Ariel Gomez[b,1], Aaron J. Kosar[c], D. Scott Bohle[c], Ernst Hempelmann[d], Diego Menezes[e], Marcos André Vannier-Santos[e], Pedro L. Oliveira[a], Sérgio T. Ferreira[a,f]

[a] *Instituto de Bioquímica Médica, Programas de Biologia Molecular e Biotecnologia, Bioquímica e Biofísica Celular, Universidade Federal do Rio de Janeiro, Cidade Universitária, Rio de Janeiro, RJ 21941-590, Brazil*
[b] *Department of Physics, MacNaughton Bldg, Gordon Street, University of Guelph, Guelph, Ont., Canada N1G 2W1*
[c] *Department of Chemistry, McGill University, 801 Sherbrooke West, Montreal, Que., Canada H3A 2K6*
[d] *Department of Parasitology, Institute of Tropical Medicine, Tübingen University, Tübingen, Germany*
[e] *Centro de Pesquisas Gonçalo Moniz, Fiocruz, Salvador, Brazil*
[f] *Laboratório Nacional de Luz Síncrotron, Caixa Postal 6192, Campinas, SP, Brazil*

Received 28 June 2005; revised 22 July 2005; accepted 5 September 2005

Available online 5 October 2005

Edited by Hans Eklund

Dedicated to the memories of Adalberto Abreu Lemos (1910–2002) and Isaura Lemos Fernandes (1913–2002).

Abstract Hemozoin (Hz) is a heme crystal produced upon the digestion of hemoglobin (Hb) by blood-feeding organisms as a main mechanism of heme disposal. The structure of Hz consists of heme dimers bound by reciprocal iron–carboxylate interactions and stabilized by hydrogen bonds. We have recently described heme crystals in the blood fluke, *Schistosoma mansoni*, and in the kissing bug, *Rhodnius prolixus*. Here, we characterized the structures and morphologies of the heme crystals from those two organisms and compared them to synthetic β-hematin (βH). Synchrotron radiation X-ray powder diffraction showed that all heme crystals share the same unit cell and structure. The heme crystals isolated from *S. mansoni* and *R. prolixus* consisted of very regular units assembled in multicrystalline spherical structures exhibiting remarkably distinct surface morphologies compared to βH. In both organisms, Hz formation occurs inside lipid droplet-like particles or in close association to phospholipid membranes. These results show, for the first time, the structural and morphological characterization of natural Hz samples obtained from these two blood-feeding organisms. Moreover, Hz formation occurring in close association to a hydrophobic environment seems to be a common trend for these organisms and may be crucial to produce very regular shaped phases, allowing the formation of multicrystalline assemblies in the guts of *S. mansoni* and *R. prolixus*.

Keywords: Hemozoin; Heme; X-ray diffraction; *Rhodnius prolixus*; *Schistosoma mansoni*

1. Introduction

Blood-feeding organisms are implicated, not only as vectors of several important infectious diseases including malaria and Chagas' disease, but also as causative agents as in schistosomiasis. These organisms usually digest large quantities of hemoglobin (Hb) to meet their nutritional requirements. During this digestive process, amino acids, peptides and heme are released [1]. Heme constitutes an essential molecule to most living organisms [2]. However, in a free state it acts as a pro-oxidant, participating in the formation of free radicals [3] and also interferes with phospholipid membrane stability, altering the bilayer structure and leading to cell disruption [4,5]. Thus, the ways in which blood-feeding organisms deal with free heme are of central importance in their physiologies. In order to overcome its toxicity, very efficient mechanisms of heme detoxification have evolved in such organisms, including the enzyme heme oxygenase [3] and heme binding proteins such as HeLp, a heme lipoprotein from the cattle tick *Boophilus microplus* [6] and RHBP, a hemolymphatic protein present in the kissing bug vector of Chagas' disease *Rhodnius prolixus* [7]. Heme can also be detoxified by its aggregation that takes place in a specialized organelle named hemosome in the cattle tick *B. microplus* [8]. In malaria parasites, a similar process occurs inside the digestive vacuole, consisting of crystallization of free heme into a dark brown pigment named hemozoin (Hz) [9,10]. We and others [11,12] have recently identified this heme crystal in other blood-feeding organisms, such as *R. prolixus*, the helminth *Schistosoma mansoni*, the main etiologic agent of human schistosomiasis [13] and the protozoan *Haemoproteus columbae* [14]. In these organisms, Hz formation seems to represent the main heme detoxification pathway. Recent findings from our group corroborate this hypothesis, as in vivo treatment of *Schistosoma*-infected mice with the antimalarial, chloroquine, inhibits Hz formation in *S. mansoni* and reduces parasite burden and egg deposition in the livers of the infected animals [15].

The structure of Hz was originally demonstrated based on synchrotron radiation X-ray powder diffraction (SR-XRD) [16] and revealed its identity to the synthetic analog, β-hematin (βH). Later, it was shown that heme monomers in βH are dimerized through reciprocal iron-carboxylate bonds involving one of the propionic side chains of each porphyrin ring, with

*Corresponding author. Fax: +55 21 22708647.
E-mail address: maroli@bioqmed.ufrj.br (M.F. Oliveira).

[1] These authors have equally contributed to this work.

0014-5793/$30.00
doi:10.1016/j.febslet.2005.09.035

neighbouring dimers forming chains stabilized through hydrogen bonds [10]. However, the structural determination of natural Hz directly obtained from blood-feeding organisms remained elusive. Recent reports indicate that a surprisingly diverse array of spectroscopically similar heme crystalline phases can be formed during βH synthesis and that infra-red spectroscopy alone, is insufficient to individually identify synthetic analogues of Hz [17]. Thus, a combination of electron microscopy and SR-XRD is required to unambiguously identify different crystalline states of heme. Given the scarcity of data available about heme crystals in *S. mansoni* and in *R. prolixus*, here we aimed to investigate the structures and morphologies of these crystals by using spectroscopic and electron microscopy techniques and by comparing them with synthetic βH.

2. Materials and methods

2.1. β-hematin

Synthetic βH was prepared following the method of dehydrohalogenation of hemin as previously described [18].

2.2. Animals and Hz extraction

Rhodnius prolixus adult females were reared with rabbit blood and kept for four days at 28 °C and 80% relative humidity. Briefly, *R. prolixus* midgut were incubated in phosphate buffered saline and gently shaken for 5 min at room temperature. The tubes were left undisturbed for 5 min to allow sedimentation of tissue debris and the supernatants were collected and subjected to Hz extraction as previously described [11]. *Schistosoma mansoni* strain LE was maintained in *Biomphalaria glabrata* snails and in syrian hamsters. Adult worms were obtained by mesenteric perfusion of hamsters 42 days after infection, as previously described [19]. Adult female worms were homogenized in phosphate buffered saline at 25 °C and subjected to Hz extraction based on previously described methods [13].

2.3. Synchrotron radiation X-ray powder diffraction

High-resolution powder diffraction data were collected at the XRD1 beamline at the National Synchrotron Light Laboratory (LNLS), Campinas, Brazil. Samples were ground in an agate mortar and spread over a glass slide so that no part of the X-ray beam would spill over the sample holder at angles as low as 6° (2θ). The sample holders were mounted on a spinning stage and carefully aligned to the center of a two-axis diffractometer. Rotation about the ω axis for fixed 2θ angles, at several diffraction peaks (2θ), demonstrated that the samples had no preferred orientation. All measurements were carried out at room temperature at a wavelength of 1.7263 Å, near the iron absorption edge to allow resonant scattering. The βH sample was additionally measured using a wavelength of 1.4644 Å, so that two independent datasets were available to check for the correctness of the structural model. Scans were performed using angular steps of 0.02° in 2θ from 6° to 55.6°.

2.4. Field emission scanning electron microscopy (FESEM)

Dry Hz or βH samples were re-suspended in deionized water and a drop of the resulting suspension was applied onto a silicon chip and kept at 37 °C until dry. Then, the samples were coated with gold for 30 s and were examined in a JEOL JSM-6340F field emission scanning electron microscope at an accelerating voltage of 5.0 kV. Images were acquired by a digital photodocumentation system.

2.5. Transmission electron microscopy (TEM)

Samples of *R. prolixus* midgut or *S. mansoni* adult females were fixed overnight at room temperature in 1% glutaraldehyde and 4% formaldehyde in 0.1 M sodium cacodylate buffer, pH 7.4. They were then rinsed and postfixed in 1% OsO4, 0.8% $K_3Fe(CN)_6$ and 5 mM $CaCl_2$ in the same buffer for 1 h. Samples were dehydrated in acetone and embedded in epoxy Polybed resin (Polyscience). Ultrathin sections were stained with uranyl acetate, lead citrate and were examined in a Zeiss 109 electron microscope. Images were acquired using a Megaview II digital system.

3. Results and discussion

High-resolution SR-XRD data were collected from *S. mansoni* and *R. prolixus* Hz as well as from synthetic βH. All the patterns gave rise to sharp Bragg diffraction peaks corresponding to crystalline materials (Fig. 1). A priori examination of peaks positions and intensities of the three SR-XRD spectra (measured at 1.7263 Å) showed that they exhibited virtually identical patterns, suggesting that the three compounds have the same crystal structure. The diffraction pattern obtained from the *S. mansoni* Hz also exhibited some contribution from an amorphous background signal, which may likely be explained by the presence of lipids or even to less crystalline amorphous Hz pigments that co-purified with the isolated Hz crystals. A similar effect of diffuse scattering background has previously been reported in SR-XRD measurements of malaria pigment in red cells infected with *Plasmodium falciparum* [16,17]. Despite the relatively lower quality of the resulting SR-XRD pattern for *S. mansoni* Hz compared to βH and *R. prolixus* Hz, cell assignment and structure determination were also carried out for this sample. Cell assignment, using the program CRYSFIRE [20], gave practically identical triclinic unit cells for both *S. mansoni* and *R. prolixus* Hz, as well as for βH (Table 1). Good de Wolf figures of merits, M [21], were obtained for βH and *R. prolixus* Hz (37.2 and 34.5, respectively). The triclinic unit cells found for these two compounds also had cell parameters very similar to those reported by Pagola et al. [10] for βH (Table 1) as refined using CELREF [22]. The excellent agreement in cell parameters for the two natural samples of *S. mansoni* and *R. prolixus* Hz and for βH suggested that the three compounds share the same structure.

Further demonstration that, at atomic level, the structures of *S. mansoni* and *R. prolixus* Hz are the same as that of βH was obtained by performing Rietveld fits of the experimental data using the atomic coordinates reported for βH [10] and refining only the cell and profile parameters. Rietveld refinements were carried out using GSAS [23] and gave very high agreement fac-

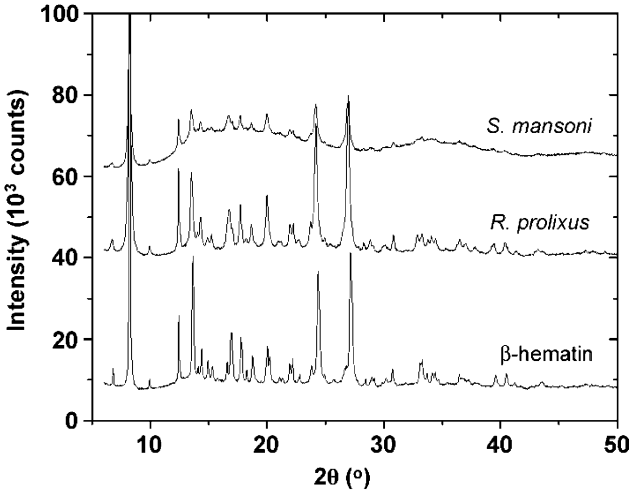

Fig. 1. X-ray powder diffraction patterns measured at 1.7263 Å for (A) *S. mansoni* Hz, (B) *R. prolixus* Hz and (C) βH.

Table 1
Unit cell parameters obtained from refinement using CELREF [22] of *S. mansoni* and *R. prolixus*Hz, and synthetic βH

	a (Å)	*b* (Å)	*c* (Å)	α (°)	*β* (°)	*γ* (°)	R_{wp} (%)
S. mansoni	12.21(2)	14.784(15)	8.034(9)	90.54(15)	97.10(12)	97.23(12)	6.9
R. prolixus	12.206(12)	14.776(8)	8.028(5)	90.48(9)	97.09(7)	97.38(7)	7.4
β-Hematin	12.198(6)	14.681(4)	8.013(3)	90.65(3)	96.74(3)	97.78(3)	6.4
β-Hematin [10]	12.196(2)	14.684(2)	8.040(1)	90.22(1)	96.80(1)	97.92(1)	6.37

Data for βH reported by Pagola et al. [10] are also shown for comparison. Scans were performed using angular steps of 0.02° in 2θ from 6° to 55.6°, as described in Section 2.

tors, $R_{wp} > 14\%$. We then used the simulated annealing program FOX [24] to look for an alternative structural model compatible with our data. In this analysis, both triclinic space groups (P1 and P$\bar{1}$) were considered and all interatomic distances and angles were restricted to the values found by Pagola et al. [10]. The porphyrin ring has 4/mmm symmetry, which makes the βH molecule prone to lying in a local minimum during the simulated annealing process. This was avoided by first finding the position of the porphyrin ring with the iron atom and then adding the carboxylate and methyl groups in all possible conformations. For each molecule, three positional, three rotational and eight torsion angle variables were then optimized. Interestingly, we found, for both *S. mansoni* and *R. prolixus* Hz, the same structure reported by Pagola et al. for βH [10]. The small differences between the unit cell parameters of *S. mansoni* or *R. prolixus* Hz and βH (observed both in our measurements and in those reported by Pagola et al. [10]) presented in Table 1 could reflect slight differences between the process of heme crystallization in vitro (in the case of β H) and those physiologically produced in the gut of *S. mansoni* and *R. prolixus*. Similar phenomena have previously been described in the comparison of synthetic magnetite (Fe_3O_4) crystals (produced in vitro) and magnetite crystals from biological origin [25]. Final Rietveld fits were performed using GSAS [23] and constraining interatomic distances. Due to its somewhat lower quality, the diffraction pattern of the *S. mansoni* Hz was fitted to the structural model obtained for the *R. prolixus* Hz, without refining the atomic positions. Background subtracted final agreement indexes were $R_{wp} = 6.9$, 7.4 and 6.4% for the *S. mansoni* Hz, *R. prolixus* Hz and βH, respectively. The refinement for the data measured at 1.4644 Å for βH gave $R_{wp} = 8.1\%$ (data not shown). Plots showing the fits between the experimental data and calculated diffraction patterns for all crystals analyzed are presented in Fig. 2. The excellent fits demonstrate that *S. mansoni* and *R. prolixus* Hz have the same crystal and molecular structures as βH. In the crystalline phase of βH, heme molecules are linked to each other, forming dimers by means of reciprocal iron-carboxylate bonds to one of the propionate side chains of the porphyrin rings (Fig. 3), as proposed before [10]. Fe–O distances measured for βH and *R. prolixus* pigment were 1.85 and 1.82 Å, respectively, which compares very well to the value of 1.898 Å reported by Pagola et al. [10]. Heme dimers are further linked by hydrogen bonds, forming chains that are held in the crystal by Van der Waals interactions. From our current data, O_{donor}–$O_{acceptor}$ distances of 2.8 and 2.7 Å were determined for βH and *R. prolixus* Hz, respectively, which are indicative of strong hydrogen bonds.

Next, we investigated the morphologies of *S. mansoni* and *R. prolixus* Hz, as previous data from our group and others indicated that these heme crystals were significantly distinct in

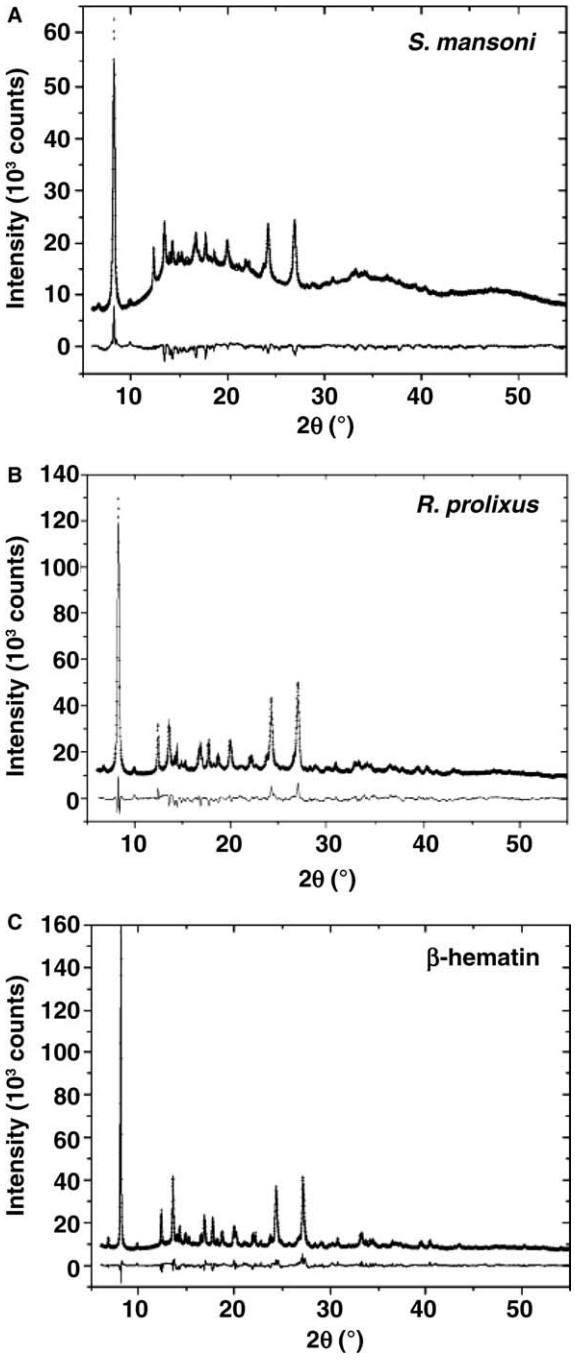

Fig. 2. Final Rietveld fits (λ = 1.7263 Å) for (A) *S. mansoni* Hz, (B) *R. prolixus* Hz and (C) synthetic βH. Experimental data points and the calculated fits are shown. The lower trace in each panel shows the difference curve.

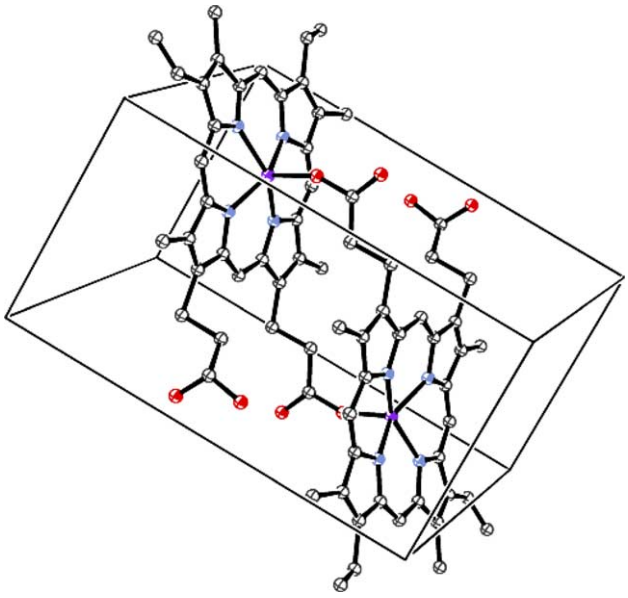

Fig. 3. Proposed unit cell structure of *R. prolixus* and *S. mansoni* Hz. The two coordinated iron atoms and the coordinating nitrogen atoms are shown in purple and blue, respectively, and the oxygen atoms of the carboxylate side chains of heme are shown in red. Two heme molecules are linked by reciprocal iron-carboxylate bonds. The structure was based on SR-XRD data for synthetic βH and for the dried Hz obtained from *R. prolixus* and *S. mansoni*, as well as on previously reported data on βH [10] (see Section 3). (For interpretation of the references to colour in this figure legend, the reader is referred to the web version of this article.)

shape from synthetic βH and *Plasmodium* Hz [11–14,17,26,27]. Field emission scanning electron microscopy (FESEM) of βH and *Plasmodium* Hz showed that these crystals were very regular in shape, with well-defined crystal facets, whereas *S. mansoni* Hz is quite heterogeneous in size, ranging from 50 nm to a few micrometers in diameter, with a roughly spherical shape [27]. Regarding *R. prolixus*, previous data from our group showed that heme crystals from this insect displayed irregular surface topography and were generally much larger than crystallites obtained from *Plasmodium* or synthetic βH [26]. Fig. 4 shows the markedly distinct morphologies that heme crystals can adopt in nature, with those obtained from *S. mansoni* and *R. prolixus* (Panels A, B and C, D, respectively), sharing more similarity between themselves than to synthetic βH crystallites (Fig. 4E). The difference in size between βH, *S. mansoni* and *R. prolixus* crystallites is probably related to the method utilized for preparing synthetic βH, as previously described [17]. A hallmark of the Hz produced by *Schistosoma* and *Rhodnius* is the apparent association between crystals, giving rise to larger roughly spherical structures composed of regularly shaped crystalline units. This can be clearly observed in higher magnification images of these crystalline assemblies (Figs. 4B and D), which show that they are composed of regular brick-shaped crystals approximately 200 nm long. Interestingly, in *S. mansoni* Hz all heme crystals were found assembled into spherical structures, whereas in *R. prolixus* heme crystals were found both in multicrystalline assemblies and as isolated approximately rod-shaped crystallites not associated with the larger structures. In sharp contrast, βH crystallites were found to be isolated species or present in non-specific clusters, with no large crystalline assemblies detected in such samples (Fig. 4E).

The multicrystalline assemblies produced by *S. mansoni* and *R. prolixus* could also be observed by transmission electron microscopy (TEM) analysis of the gut contents of those organisms (Fig. 5). Interestingly, in *S. mansoni* both crystal growth and association into larger assemblies appear to take place at the surface of electron-lucent round structures, closely resembling lipid droplets (Fig. 5A). The process of Hz formation seems to occur from the surface of this lipid droplet-like particle to its core, as observed in images of multicrystalline assemblies at different stages of crystallization (Fig. 5B). In *R. prolixus*, crystals were found both associated to vesicles derived from perimicrovillar membranes, which are phospholipid bilayer membranes that ensheath the epithelial midgut cells, and free in the midgut lumen or in multicrystalline assemblies (Fig. 5C).

Despite the fact that the resulting crystals share the same molecular structure of Hz, the results presented here indicate that Hz formation in *S. mansoni* and *R. prolixus* is different from the crystallization that takes place in *P. falciparum*. Not only are heat-labile reactions involved in Hz formation in *Schistosoma* and *Rhodnius* [12,15], but also the ultrastructural organization of the crystallites in *S. mansoni* and in *R. prolixus* (Figs. 4 and 5) are quite distinct from the ones that have been reported for *Plasmodium* Hz. In this regard, it is interesting to note that Hb digestion in *Plasmodium* is intracellular, whereas in *S. mansoni* and in *R. prolixus* digestion proceeds extracellularly. In this scenario, it is conceivable that proteins, lipids or other types of hydrophobic components or structures present in the guts of *S. mansoni* and *R. prolixus* could not only initiate heme crystallization, producing the regularly shaped crystals similar to those of *Plasmodium*, but also allowing them to interact with each other resulting in multicrystalline assemblies (Figs. 4 and 5). Such catalytic structures could act by providing a suitable site of attachment for free heme or, alternatively, a microenvironment in which heme remains soluble in an acidic milieu, a pre-requisite for the production of regular shaped crystals of Hz [17]. This possibility appears quite plausible as both lipid droplet-like particles (in *S. mansoni*) and perimicrovillar membrane-derived vesicles (in *R. prolixus*) are hydrophobic. Due to its amphipathic nature [4,5], heme could thus associate with such hydrophobic environments, allowing for the slow growth of regularly shaped Hz crystals. In this regard, preliminary data from our group show that lipid droplet-like particles isolated from *S. mansoni* females catalyze Hz formation in heat-resistant reactions, closely resembling the activity found in *P. falciparum* food vacuoles and indicating that lipids would be important catalysts of heme crystallization in *S. mansoni* (data not shown; see also [28–32]).

Regarding the mechanisms involved in Hz formation, three different possibilities have been proposed. First, histidine rich protein-II (HRP-II) was shown to be one of the catalysts in *Plasmodium* [33] but later it was argued that the histidine residues of HRP-II could not be responsible for catalyzing Hz formation due to pH restrictions in the food vacuole [34]. Moreover, parasites lacking the genes coding for HRP-II or III are still capable to produce Hz [35]. Autocatalysis was also proposed as a mechanism of Hz formation, based on the observation that purified βH could itself promote Hz growth [36]. The third possible catalyst would be lipids, especially free fatty

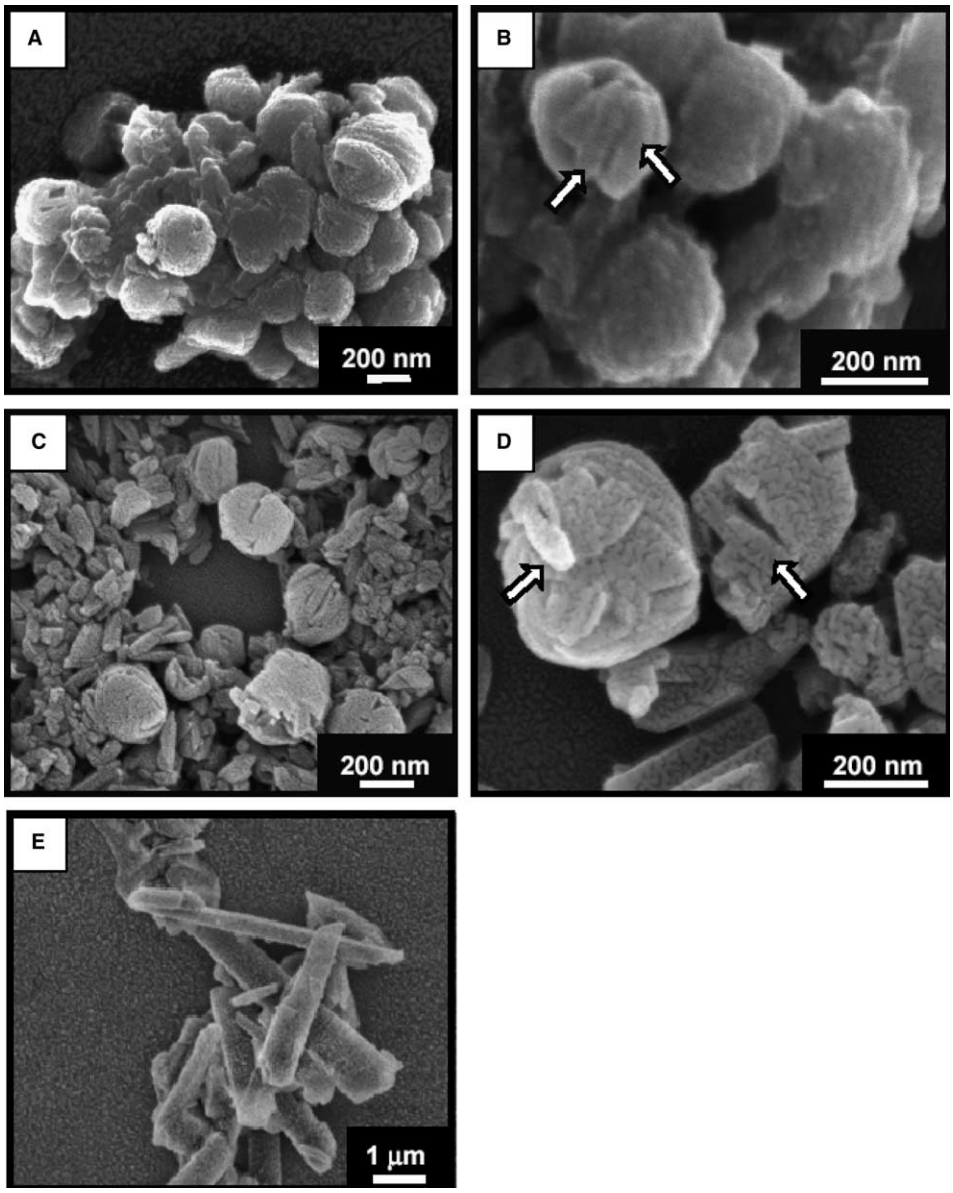

Fig. 4. Field emission scanning electron microscopy of heme crystals isolated from *S. mansoni* (A,B), *R. prolixus* (C,D) and synthetic βH (E). Arrows indicate individual Hz crystals assembled in multicrystalline structures.

acids, which would act by increasing heme solubility in acidic environments, by-passing the rate-limiting step of heme crystallization [28–31]. Interestingly, three out of four known organisms capable of producing Hz promote heme crystallization in close association to hydrophobic structures such as the food vacuole membranes in *Plasmodium* [31], the perimicrovillar membranes in *Rhodnius* [12] and lipid droplet-like particles in *Schistosoma* [32]; this study and additional unpublished data].

In *Plasmodium*, heme accumulates to millimolar concentrations inside the food vacuole, thus favouring its crystallization into Hz, which was found to be associated with membrane fractions [31]. Similarly, in the guts of *S. mansoni* and *R. prolixus* heme concentrates to the millimolar range in close association with hydrophobic/membranous components, such as lipid droplet-like particles (Figs. 5A and B; [32]) and vesicles derived from perimicrovillar membranes (Figs. 5C and D; [12]). In this context, it is possible that, inside a lipid droplet or a membrane bilayer, heme concentrates and crystallizes, producing regular shaped crystalline phases. Thus, the differences in external appearance of Hz crystals obtained from different organisms do not seem to be derived from distinct atomic structures, but rather to be generated from differences in crystal growth conditions. This suggests that the process of Hz formation in *S. mansoni* and *R. prolixus* is similar to that of *Plasmodium* parasites, since all of them produce very regular crystals exhibiting identical unit cell parameters and structures. However, for those organisms in which heme crystallization occurs extracellularly, an additional step occurs consisting of the association between crystals in larger multicrystalline assemblies, the ultimate form by which heme is eliminated. Interestingly, membranes surrounding bacterial magnetosomes have also been detected as thin halos around fossil chains of magnetite crystals, suggesting a putative catalytic role of hydrophobic environments in general biomineralization processes [37].

Heme is clearly more soluble than Hz in acidic medium and all studies on Hz formation so far have been carried out under

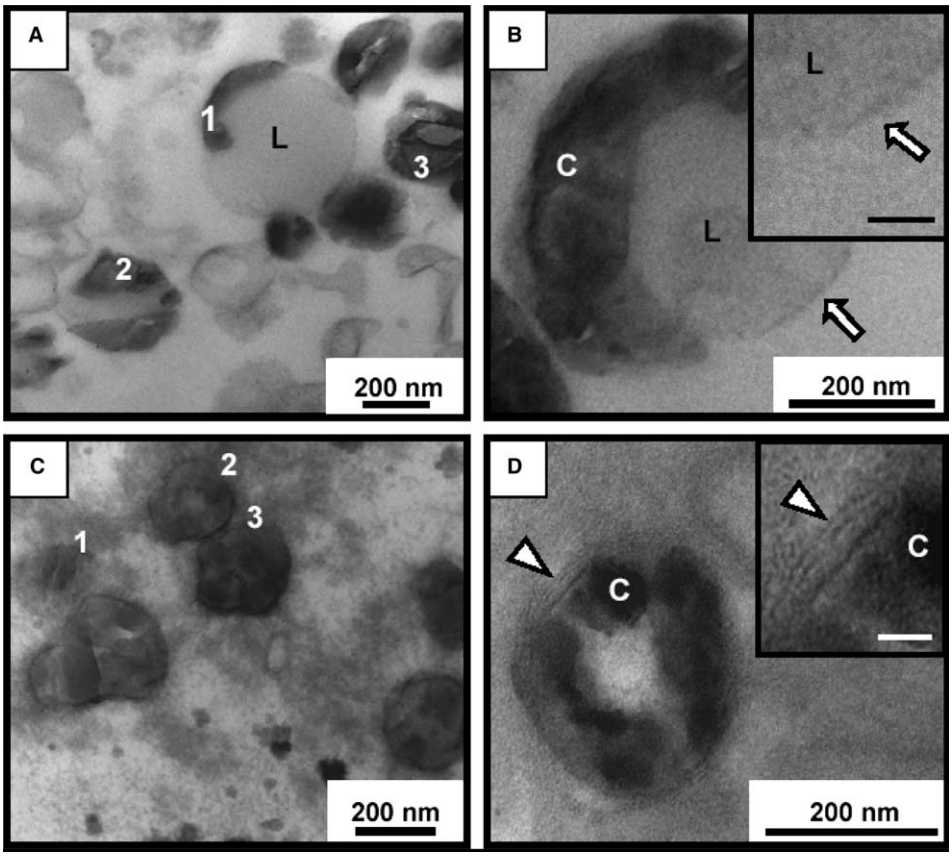

Fig. 5. Transmission electron microscopy of heme crystals observed in the luminal gut content of *S. mansoni* (A,B) and *R. prolixus* (C,D). Panel A shows the gut content of *S. mansoni*, with crystalline assemblies at three different stages of formation: initial (1), intermediate (2) and final (3); C, crystal; L, lipid droplet-like particles. Arrows in B indicate the absence of a phospholipid double membrane in a lipid droplet-like particle. Inset in B shows a lipid droplet-like particle at higher magnification. Bar = 25 nm. Panel C shows the gut content of *R. prolixus,*with crystalline assemblies at three different stages of formation: initial (1), intermediate (2) and final (3). Arrowheads in D indicate the presence of a phospholipid double membrane in perimicrovillar membranes. Inset in D shows the perimicrovillar membranes at higher magnification. Bar = 25 nm.

conditions that apparently exceed the solubility limit of heme [38]. This means that there is probably a rapid precipitation of amorphous heme, which then converts to Hz. On the other hand, in blood-feeding organisms, Hz is presumably formed from a steady-state pool of heme released as a result of continuous Hb digestion. Conceivably, the main role of all catalysts of heme crystallization so far studied is to increase the solubility of heme in acidic medium. Indeed, previous observations indicated that certain solvents, such as ethanol and benzoic acid, can enhance Hz formation [38–40]. This is further reinforced by recent findings of Egan et al. [40], who proposed that heme crystallization was more correctly understood as a biomineralization process based on the observation that, in acidic medium, acetate promotes the solubilization of sedimented heme. Under these conditions, acetate would displace the axial water bound to the central heme iron, allowing solubilization of heme [40]. Thus, it is tempting to speculate that the molecules directly involved in Hz formation in *S. mansoni* and *R. prolixus* would be present in the lipid droplet-like particles and in perimicrovillar membrane-derived vesicles, respectively. This possibility is currently being investigated in our laboratory.

In conclusion, we show that structural and morphological characterization of heme crystals produced by *S. mansoni* and *R. prolixus* provides important information concerning the assembly of heme crystals, opening new perspectives for drug development against schistosomiasis and Chagas' disease transmission. In particular, due to the structural identity of the Hz found in different species, it is possible that compounds that are currently known to interfere with heme crystallization in *Plasmodium* may be used for targeting this heme detoxification pathway in other blood-feeding organisms.

Acknowledgements: We are indebted to Drs. Marcia Attias and Kildare Miranda from Instituto de Biofísica Carlos Chagas Filho at UFRJ for the kind support on FESEM images and to Dr. Franklin D. Rumjanek from the Instituto de Bioquímica Médica at UFRJ for the *S. mansoni* maintainance facility. We are also grateful to João V. de Oliveira Neto, José de S. L. Junior, Litiane M. Rodrigues, Maria Marta Freire and Claudio P. Figueira for excellent technical assistance and to Drs. Ednildo A. Machado and Flávio A. Lara for their valuable contributions and helpful discussions. Supported by Associação Brasileira de Tecnologia de Luz Síncrotron (ABTLuS) through Project XRD917/01, CNPq, FAPERJ, PRONEX, PADCT, CAPES and the Third World Academy of Sciences (TWAS). M.F.O. and M.A.V.S. are research scholars from CNPq. P.L.O. and S.T.F. are Howard Hughes Medical Institute International Research Scholars.

References

[1] Francis, S.E., Sullivan Jr., D.J. and Goldberg, D.E. (1997) Hemoglobin metabolism in the malaria parasite *Plasmodium falciparum*. Annu. Rev. Microbiol. 51, 97–123.

[2] Ponka, P. (1999) Cell biology of haem. Am. J. Med. Sci. 318, 241–256.
[3] Ryter, S.W. and Tyrrel, R.M. (2000) The haem synthesis and degradation pathways: role in oxidant sensitivity. Haem oxygenase has both pro- and antioxidant properties. Free. Rad. Biol. Med. 28, 289–309.
[4] Chou, A.C. and Fitch, C.D. (1981) Mechanism of hemolysis induced by ferriprotoporphyrin IX. J. Clin. Invest. 68, 672–677.
[5] Schmitt, T.H., Frezzatti Jr., W.A. and Schreier, S. (1993) Hemin-induced lipid membrane disorder and increased permeability: a molecular model for the mechanism of cell lysis. Arch. Biochem. Biophys. 307, 96–103.
[6] Maya-Monteiro, C.M., Daffre, S., Logullo, C., Lara, F.A., Alves, E.W., Capurro, M.L., Zingali, R., Almeida, I.C. and Oliveira, P.L. (2000) HeLp, a heme lipoprotein from the hemolymph of the cattle tick, *Boophilus microplus*. J. Biol. Chem. 275, 36584–36589.
[7] Dansa-Petretski, M., Ribeiro, J.M., Atella, G.C., Masuda, H. and Oliveira, P.L. (1995) Antioxidant role of *Rhodnius prolixus* haem-binding protein. Protection against haem-induced lipid peroxidation. J. Biol. Chem. 270, 10893–10896.
[8] Lara, F.A., Lins, U., Paiva-Silva, G., Almeida, I.C., Braga, C.M., Miguens, F.C., Oliveira, P.L. and Dansa-Petretski, M. (2003) A new intracellular pathway of haem detoxification in the midgut of the cattle tick *Boophilus microplus*: aggregation inside a specialized organelle, the hemosome. J. Exp. Biol. 206, 1707–1715.
[9] Slater, A.F.G., Swiggard, W.J., Orton, B.R., Flitter, W.D., Goldberg, D.E., Cerami, A. and Henderson, G.B. (1991) An iron-carboxylate bond links the haem units of malaria pigment. Proc. Natl. Acad. Sci. USA 88, 325–329.
[10] Pagola, S., Stephens, P.W., Bohle, D.S., Kosar, A.D. and Madsen, S.K. (2000) The structure of malaria pigment β-haematin. Nature 404, 307–310.
[11] Oliveira, M.F., Silva, J.R., Dansa-Petretski, M., de Souza, W., Lins, U., Braga, C.M.S., Masuda, H. and Oliveira, P.L. (1999) Haem detoxification by an insect. Nature 400, 517–518.
[12] Oliveira, M.F., Silva, J.R., Dansa-Petretski, M., de Souza, W., Braga, C.M.S., Masuda, H. and Oliveira, P.L. (2000) Haemozoin formation in the midgut of the blood sucking insect *Rhodnius prolixus*. FEBS Lett. 477, 95–98.
[13] Oliveira, M.F., d'Avila, J.C.P., Torres, C.R., Oliveira, P.L., Tempone, A.J., Rumjanek, F.D., Braga, C.M.S., Silva, J.R., Petretski, M.D., Oliveira, M.A., Souza, W. and Ferreira, S.T. (2000) Haemozoin in *Schistosoma mansoni*. Mol. Biochem. Parasitol. 111, 217–221.
[14] Chen, M.M., Shi, L. and Sullivan Jr., D.J. (2001) Haemoproteus and *Schistosoma* synthesize haem polymers similar to *Plasmodium* hemozoin and beta-hematin. Mol. Biochem. Parasitol. 113, 1–8.
[15] Oliveira, M.F., d'Avila, J.C.P., Tempone, A.J., Soares, J.B.R., Rumjanek, F.D., Ferreira-Pereira, A., Ferreira, S.T. and Oliveira, P.L. (2004) Inhibition of heme aggregation by chloroquine reduces *Schistosoma mansoni* infection. J. Infect. Dis. 190, 843–852.
[16] Bohle, D.S., Dinnebier, R.E., Madsen, R.K. and Stephens, P.W. (1997) Characterization of the products of the haem detoxification pathway in malarial late trophozoites by X-ray diffraction. J. Biol. Chem. 272, 713–715.
[17] Bohle, D.S., Kosar, A.D. and Stephens, P.W. (2002) Phase homogeneity and crystal morphology of the malaria pigment beta-hematin. Acta Crystallogr. D. Biol. Crystallogr. 58, 1752–1756.
[18] Bohle, D.S. and Helms, J.B. (1993) Synthesis of beta-hematin by dehydrohalogenation of hemin. Biochem. Biophys. Res. Commun. 193, 504–508.
[19] Smithers, S.R. and Terry, R.J. (1965) The infection of laboratory hosts with cercariae of *Schistosoma mansoni* and the recovery of adult worms. Parasitology 55, 695–700.
[20] Shirley, R. (2002) The Crysfire 2002 System for Automatic Powder Indexing: User's Manual, The Lattice Press, 41 Guildford Park Avenue, Guildford, Surrey GU2 7NL, England.
[21] Wolff, P.M.D. (1968) A simplified criterion for the reliability of a powder pattern indexing. J. Appl. Cryst. 1, 108–113.
[22] Laugier, J., Bochu, B., *LMGP-Suite* of programs for the interpretation of X-ray Experiments, Laboratoire des Matériaux et du Génie Physique, Ecole Nationale Supérieure de Physique de Grenoble, BP 46. 38042 Saint Martin d'Hères, France. Available from <http://www.inpg.fr/LMGP> and <http://www.ccp14.ac.uk/tutorial/lmgp/>.
[23] Larson, A.C. and von Dreele, R.B. (2000) General Structure Analysis System (GSAS), Los Alamos National Laboratory Report LAUR, 86-748.
[24] Favre-Nicolin, V. and Cerný, R. (2002) FOX, 'free objects for crystallography': a modular approach to ab initio structure determination from powder diffraction. J. Appl. Cryst. 35, 734–743.
[25] Thomas-Keprta, K.L., Clemett, S.J., Bazylinski, D.A., Kirschvink, J.L., McKay, D.S., Wentworth, S.J., Vali, H., Gibson Jr., E.K., McKay, M.F. and Romanek, C.S. (2001) Truncated hexa-octahedral magnetite crystals in ALH84001: presumptive biosignatures. Proc. Natl. Acad. Sci. USA 98, 2164–2169.
[26] Oliveira, M.F., Timm, B.L., Machado, E.A., Miranda, K., Attias, M., Silva, J.R., Dansa-Petretski, M., de Oliveira, M.A., de Souza, W., Pinhal, N.M., Sousa, J.J., Vugman, N.V. and Oliveira, P.L. (2002) On the pro-oxidant effects of haemozoin. FEBS Lett. 512, 139–144.
[27] Noland, G.S., Briones, N. and Sullivan Jr., D.J. (2003) The shape and size of hemozoin crystals distinguishes diverse Plasmodium species. Mol. Biochem. Parasitol. 130, 91–99.
[28] Bendrat, K., Berger, B.J. and Cerami, A. (1995) Haem polymerization in malaria. Nature 378, 138–139.
[29] Dorn, A., Vippagunta, S.R., Matile, H., Bubendorf, A., Vennerstrom, J.L. and Ridley, R.G. (1998) A comparison and analysis of several ways to promote haematin (haem) polymerisation and an assessment of its initiation in vitro. Biochem. Pharmacol. 55, 737–747.
[30] Fitch, C.D., Cai, G.Z., Chen, Y.F. and Shoemaker, J.D. (1999) Involvement of lipids in ferriprotoporphyrin IX polymerization in malaria. Biochim. Biophys. Acta 1454, 31–37.
[31] Hempelmann, E., Motta, C., Hughes, R., Ward, S.A. and Bray, P.G. (2003) *Plasmodium falciparum*: sacrificing membrane to grow crystals?. Trends Parasitol. 19, 23–26.
[32] Sodeman, T.M., Sodeman Jr., W.A. and Schnitzer, B. (1972) Lamellar structures in the gut of *Schistosoma haematobium*. Ann. Trop. Med. Parasitol. 66, 475–478.
[33] Sullivan, D.J., Gluzman, I.Y. and Goldberg, D.E. (1996) *Plasmodium* hemozoin formation mediated by histidine-rich proteins. Science 271, 219–221.
[34] Lynn, A., Chandra, S., Malhotra, P. and Chauhan, V.S. (1999) Heme binding and polymerization by *Plasmodium falciparum* histidine rich protein II: influence of pH on activity and conformation. FEBS Lett. 459, 267–271.
[35] Sullivan, D.J. (2002) Theories on malarial pigment formation and quinoline action. Int. J. Parasitol. 32, 1645–1653.
[36] Dorn, A., Stoffel, R., Matile, H., Bubendorf, A. and Ridley, R.G. (1995) Malarial haemozoin/beta-haematin supports haem polymerization in the absence of protein. Nature 374, 269–271.
[37] Gorby, Y.A., Beveridge, T.J. and Blakemore, R.P. (1988) Characterization of the bacterial magnetosome membrane. J. Bacteriol. 170, 834–841.
[38] Egan, T.J. (2002) Physico-chemical aspects of hemozoin (malaria pigment) structure and formation. J. Inorg. Biochem. 91, 19–26.
[39] Blauer, G. and Akkawi, M. (2002) Alcohol-water as a novel medium for beta-hematin preparation. Arch. Biochem. Biophys. 398, 7–11.
[40] Egan, T.J., Mavuso, W.M. and Ncokazi, K.K. (2001) The mechanism of β -hematin formation in acetate solution. Parallels between hemozoin formation and biomineralization processes. Biochemistry 40, 204–213.